α-decay spectroscopy of the $N = 130$ isotones ^{218}Ra and ^{220}Th: mitigation of α-particle energy summing with implanted nuclei

E. Parr*,[1,2,†] J. F. Smith,[1,2] P. T. Greenlees,[3] K. Auranen,[3] P. A. Butler,[4] R. Chapman,[1,2] D. M. Cox,[3] D. M. Cullen,[5] L. P. Gaffney‡,[1,2] T. Grahn,[3] E. T. Gregor,[1,2] L. Grocutt,[1,2] A. Herzáň§,[3] R.-D. Herzberg,[4] D. Hodge,[5] U. Jakobsson,[3] R. Julin,[3] S. Juutinen,[3] J. Keatings,[1,2] J. Konki¶,[3] M. Leino,[3] P. P. McKee,[1,2] C. McPeake,[4] D. Mengoni,[6] A. K. Mistry,[4] K. F. Mulholland,[1,2] B. S. Nara Singh**,[5] G. G. O'Neill,[4] J. Pakarinen,[3] P. Papadakis††,[3] J. Partanen,[3] P. Peura,[3] P. Rahkila,[3] P. Ruotsalainen,[3] M. Sandzelius,[3] J. Sarén,[3] M. Scheck,[1,2] C. Scholey,[3] M. Siciliano‡‡,[3] M. Smolen,[1,2] J. Sorri§§,[3] P. Spagnoletti,[1,2] K. M. Spohr,[1,2] S. Stolze¶¶,[3] M. J. Taylor***,[5] and J. Uusitalo[3]

[1]*School of Computing, Engineering, and Physical Sciences, University of the West of Scotland, Paisley, PA1 2BE, United Kingdom*
[2]*Scottish Universities Physics Alliance*
[3]*University of Jyvaskyla, Department of Physics, P.O. Box 35, FI-40014 University of Jyvaskyla, Finland*
[4]*Oliver Lodge Laboratory, University of Liverpool, Liverpool, L69 7ZE, United Kingdom*
[5]*School of Physics and Astronomy, Schuster Building, University of Manchester, Manchester, M13 9PL, United Kingdom*
[6]*Dipartimento di Fisica e Astronomia dell' Università and INFN Sezione di Padova, Padova, Italy*

(Dated: September 10, 2019)

An analysis technique has been developed in order to mitigate energy summing due to sequential short-lived α decays from nuclei implanted into a silicon detector. Using this technique, α-decay spectroscopy of the $N = 130$ isotones ^{218}Ra ($Z = 88$) and ^{220}Th ($Z = 90$) has been performed. The energies of the α particles emitted in the ^{218}Ra$\rightarrow^{214}$Rn and ^{220}Th$\rightarrow^{216}$Ra ground-state to ground-state decays have been measured to be 8381(4) keV and 8818(13) keV, respectively. The half-lives of the ground states of ^{218}Ra and ^{220}Th have been measured to be 25.99(10) μs and 10.4(4) μs, respectively. The half-lives of the ground states of the α-decay daughters, ^{214}Rn and ^{216}Ra have been measured to be 259(3) ns and 161(11) ns, respectively. Fine structure in the α decay of ^{218}Ra has been observed for the first time, populating the 695-keV 2_1^+ state in ^{214}Rn. The fine-structure α decay has an α-particle energy of 7715(40) keV, and branching ratio $b_\alpha = 0.123(11)\%$.

PACS numbers: 23.60.+e, 27.80.+w, 29.30.Ep, 29.30.Kv

*Present address: Oliver Lodge Laboratory, University of Liverpool, Liverpool, L69 7ZE, United Kingdom
‡Present address: Oliver Lodge Laboratory, University of Liverpool, Liverpool, L69 7ZE, United Kingdom
§Present address: Institute of Physics, Slovak Academy of Sciences, SK-84511 Bratislava, Slovakia
¶Present address: CERN, CH-1211 Geneva 23, Switzerland
**Present address: School of Computing, Engineering, and Physical Sciences, University of the West of Scotland, Paisley, PA1 2BE, United Kingdom
††Present address: Nuclear Physics Group, STFC Daresbury Laboratory, Daresbury, Warrington WA4 4AD, United Kingdom
‡‡Present address: Dipartimento di Fisica e Astronomia, Universitá di Padova, I-35131 Padova, Italy
§§Present address: Sodankylä Geophysical Observatory, University of Oulu, Sodankylä, Finland
¶¶Present address: Physics Division, Argonne National Laboratory, Argonne, Illinois 60439, USA
***Division of Cancer Sciences, School of Medical Sciences, The University of Manchester, Manchester, M13 9PL, UK
†Electronic address: ep@ns.ph.liv.ac.uk

CORRESPONDING AUTHOR:
Dr Edward Parr

(Present) Address:
Nuclear Physics Group,
Oliver Lodge Laboratory,
University of Liverpool,
Liverpool, L69 7ZE,
United Kingdom
Email: ep@ns.ph.liv.ac.uk

I. INTRODUCTION

Alpha-decay spectroscopy is a well-established technique in nuclear physics; it provides valuable data about nuclear structure and properties, often for nuclei that are otherwise difficult to study. Knowledge of the α-particle energy, or Q value, alone gives a direct measurement of the relative masses of mother and daughter nuclei. Fine structure in α decay can help to identify final states in the daughter nuclei; branching ratios of different α decays from the same state can provide information about nuclear structure [1]. To this end, it is often useful to define the hindrance factor of an α decay [2, 3], which can give a measure of the overlap of the wavefunctions of initial and final states involved in the decay. In practice, α-decay spectroscopy can be very challenging for some nuclei due to small production cross sections or small branching ratios associated with decays between structurally-different states, or to final states with high excitation energy in the daughter nucleus. Also, if the α decay under study is part of a chain of sequential α decays, subsequent short-lived α decays can give rise to technical difficulties; for example, if the half-life of a subsequent decay is less than the detector response time, the detector may still be processing the first α-particle signal when the second is received. This can result in pile-up, giving a composite energy signal that is difficult to deconvolve. The value of α-decay data is such that it is important to develop new experimental and analysis methods that can mitigate some of these problems.

The $N = 130$ nuclei from $Z = 86$ (^{216}Rn) to $Z = 93$ (^{223}Np) decay by α-particle emission. The $N = 128$ ($84 \leq Z \leq 91$) daughter nuclei themselves then decay by α-particle emission to daughter nuclei with a closed $N = 126$ shell, with half-lives of less than 300 ns in all cases. In α-decay spectroscopy, a consequence of such short half lives is that α particles emitted from the $N = 130$ nuclei are likely to be detected together with α particles from the $N = 128$ daughter, as a single piled-up event. This makes measurements of the α particle energies and half-lives very difficult. For the $N = 130$ nuclei, these problems are exacerbated by the fact that the production cross sections are low due to the lack of available stable beam and target combinations for fusion-evaporation reactions, and due to the propensity for fission of the high-Z compound nuclei. Despite these problems, α-decay spectroscopy of some of the $N = 130$ nuclei has previously been carried out; ground-state to ground-state α decays have been identified, but often with large uncertainties on the measured energies. In the early 1970s some studies were carried out using catcher-foil methods; essentially two methods were employed, one using a helium gas-jet to slow reaction products before depositing them on a catcher foil, and the other using direct implantation into a foil. In the helium gas-jet method, the parent of the nucleus of interest was deposited on the catcher foil, so that method could only be used where the half-life of the parent was sufficiently long. This was used to study the α decay of $^{216}_{86}$Rn [4], $^{217}_{87}$Fr [5], $^{218}_{88}$Ra [4, 6], and $^{219}_{89}$Ac [5]. When the half-life is short, an alternative method using direct implantation into a catcher foil has been used; this was the case for the study of the α decay of $^{220}_{90}$Th [7]. In these methods α-particle energies were measured using detectors placed near the foils. These methods were very useful for studying ground-state to ground-state α decays where the cross-sections and branching ratios were relatively large. However, they were not suitable for studying α decays from nuclei produced with low cross sections, in amongst a background of more intense reaction products, or for weak fine-structure α-decay branches. An alternative to the catcher-foil method was introduced by Hingmann *et al.* [8] in 1983, in which the nuclei of interest were implanted into a silicon detector, which itself subsequently detected α particles that were emitted from the implanted nucleus; this method was used to identify α decays from ^{221}Pa and ^{222}U [8]. Although the method was successful in measuring the half-lives of the decays, it was not possible to accurately measure the α-particle energies due to energy summing from the $N = 130$ and $N = 128$ decays. An attempt was made to infer the α-particle decay energy in ^{221}Pa [9] from sum-energy peaks, but the method resulted in a large associated uncertainty. More recently, digital pulse-shape analysis techniques have been used to measure α-particle energies for nuclei that have α-decay daughter nuclei with sub-microsecond half-lives [10]. This method has notably been used in the α-decay spectroscopy of nuclei around ^{100}Sn, with the α-particle energies from the ^{109}Xe$\rightarrow^{105}$Te$\rightarrow^{101}$Sn decay chain being measured with high precision [11–13] and the ^{108}Xe$\rightarrow^{104}$Te$\rightarrow^{100}$Sn chain being identified recently for the first time [14]. Digital pulse shapes have also been used to measure the α-particle energies from the highest-mass $N = 130$ isotones ^{222}U [15] and ^{223}Np [16]; however, in these cases, there are significant uncertainties on the measured energies. The inability to identify weaker α-decay branches using catcher-foil methods and the complications arising from energy summing inherent in implantation methods mean that no fine structure has, to date, been observed in any of the eight $N = 130$ nuclei from ^{216}Rn ($Z = 86$) to ^{223}Np ($Z = 93$).

The $N = 130$ $^{216}_{86}$Rn, $^{217}_{87}$Fr, $^{218}_{88}$Ra, $^{219}_{89}$Ac, $^{220}_{90}$Th, $^{221}_{91}$Pa, $^{222}_{92}$U, and $^{223}_{93}$Np isotones lie in the transitional region between the spherical nuclei above ^{208}Pb and the well-deformed nuclei around ^{226}Ra. Some of these nuclei lie on the low-N edge of the light-actinide octupole-deformed region [17]. Experimental study of the α decay of these nuclei can provide useful information about the development of octupole collectivity as a function of N and Z as discussed in Refs. [18–20]. However, the α-decay spectroscopy of these nuclei is difficult due to their short-lived daughter nuclei, as discussed above. In the present work, α-decay spectroscopy of $N = 130$ isotones ^{218}Ra and ^{220}Th has been carried out. Nuclei produced in fusion-evaporation reactions have been implanted into a silicon detector at the focal plane of the RITU recoil separa-

tor at the JYFL Accelerator Laboratory at the University of Jyväskylä in Finland. The implantation detector was surrounded by separate PIN-diode detectors which were used to detect α particles that escape from the implantation detector, thereby helping to reduce energy summing. The α-decay chains $^{218}_{88}$Ra$\rightarrow^{214}_{86}$Rn$\rightarrow^{210}_{84}$Po and $^{220}_{90}$Th$\rightarrow^{216}_{88}$Ra$\rightarrow^{212}_{86}$Rn have hence been studied using these methods. The ground-state to ground-state α decays of ^{218}Ra and ^{220}Th have been studied and the α-particle energies have been measured. Fine structure in the α decay of ^{218}Ra has been observed for the first time populating the 2^+_1 state in ^{214}Rn, and the α-particle energy and branching ratio have been measured.

II. PREVIOUS STUDIES

The measurements in this work are focused on the α decay of the $N = 130$ isotones ^{218}Ra and ^{220}Th. The ^{218}Ra$\rightarrow^{214}$Rn ground-state to ground-state α decay has been reported several times. In 1970, Valli *et al.,* [4] and Torgerson *et al.,* [6] used catcher-foil methods with a helium gas-jet. Later, in 1986, Kim *et al.,* [21] implanted ^{218}Ra fusion-evaporation products into a silicon detector and the α-particle energy was inferred from the sum peaks that were recorded. The energies of the α particles measured by Valli *et al.* [4] and Torgerson *et al.* [6] were 8385(10) keV and 8392(8) keV, respectively, which are consistent with each other but that measured by Kim *at al.* [21] is almost 100 keV larger with a value of 8480(20) keV. The half-life of ^{218}Ra was measured to be 14(2) μs by Valli *et al.* [4], but was later consistently measured with higher values of 25.6(11) μs by Toth *et al.* [22], 26(2) μs by Wieland *et al.* [23] and 25.2(3) μs by Kuusiniemi *et al.* [24]. The half-life of the ^{214}Rn ground state populated in the ^{218}Ra$\rightarrow^{214}$Rn α decay has been measured with values of 270(20) ns by Valli *et al.* [4] and 263(35) ns by Dracoulis *et al.* [25].

The energy of the α particle emitted in the ^{220}Th$\rightarrow^{216}$Ra ground-state to ground-state decay has only previously been measured once, by Häusser *et al.* in 1973 [7], where it was reported with a value of 8790(20) keV. In that work, the half-life of the ground state of ^{220}Th was measured to be 9.7(6) μs. A measurement of the half-life was also reported by Andreev *et al.* in Ref. [26], giving a value of 12^{+4}_{-3} μs. The half-life of the ^{216}Ra ground state populated in the ^{220}Th$\rightarrow^{216}$Ra α decay has been reported by Nomura *et al.* [27] to be 182(10) ns.

III. EXPERIMENTAL DETAILS

The results presented here are taken from two experiments that were performed at the Accelerator Laboratory of the University of Jyväskylä in Finland. The details of the experiments are summarised in Table I. The first experiment (denoted as Experiment 1 in Table I) used an ^{18}O beam incident on a ^{208}Pb target, and was optimised to study the nucleus ^{222}Th produced via the ^{208}Pb(^{18}O,$4n$)^{222}Th fusion-evaporation reaction. The second experiment (Experiment 2) essentially swapped the ^{18}O beam for ^{20}Ne, and was optimised for the study of ^{224}U, also produced by $4n$ evaporation. The ^{218}Ra and ^{220}Th nuclei of interest in the present paper were produced as the α-decay daughters of the main ^{222}Th and ^{224}U reaction products, respectively. Both experiments used the same experimental set-up, which is described below. In both experiments the target was located at the centre of the SAGE spectrometer [28], which was used to detect prompt γ rays and internal-conversion electrons; however, data from the SAGE spectrometer are not presented in this paper. Downstream of the target, recoiling evaporation residues were separated from fission fragments and unreacted beam ions using the RITU gas-filled recoil separator [29, 30] and were transported to its focal plane. At the focal-plane of RITU, the reaction products and their subsequent decays were further studied with a suite of detectors, including double-sided silicon-strip detectors (DSSDs), PIN-diode detectors, and clover HPGe detectors, which are part of the GREAT spectrometer [31]. The reaction products were implanted into one of two DSSDs placed side-by-side at a focal plane. The DSSDs each consisted of 40 horizontal strips and 60 vertical strips giving a total of 4800 individual pixels. An array of 28 silicon PIN-diode detectors was located in front (upstream) of the DSSDs, and was used to detect charged particles emitted from nuclei implanted into the DSSDs. In standard operation, a multi-wire proportional counter (MWPC) is placed in front (upstream) of the DSSD/PIN-diode detectors; the purpose of the MWPC is to provide energy-loss and time-of-flight information to help distinguish between evaporation residues and scattered beam. However, in the present experiments the MWPC was not used due to the low energies of the evaporation residues, so in the present work time-of-flight information was extracted from the DSSD signals; more specifically the time of flight was measured as the time between prompt signals in SAGE and the subsequent corresponding (implantation) signal in the DSSDs. For the detection of X rays and γ rays emitted from implanted nuclei, three clover HPGe detectors were placed around the DSSDs. Relative to the central ion trajectory, the centres of the clover detectors had polar coordinates (θ, ϕ) of $(90°, 0°)$, $(90°, 90°)$ and $(90°, 270°)$, where $\phi = 0°$ is defined to be vertically upwards. In summary, the detectors of the GREAT spectrometer provide the capability to detect the evaporation residues and their subsequent charged-particle and γ-ray decays.

The data presented in this paper are focused on the $^{222}_{90}$Th$\rightarrow^{218}_{88}$Ra$\rightarrow^{214}_{86}$Rn$\rightarrow^{210}_{84}$Po and $^{224}_{92}$U$\rightarrow^{220}_{90}$Th$\rightarrow^{216}_{88}$Ra$\rightarrow^{212}_{86}$Rn α-decay chains and are taken from the DSSDs, PIN-diode detectors, and clover HPGe detectors at the focal plane of RITU. The α particles emitted from the nuclei implanted into the DSSDs were detected within the DSSDs themselves and

in the PIN-diode detectors, and γ rays emitted from states populated in the daughter nuclei were detected by the focal-plane clover HPGe detectors. Of particular relevance to the analysis and results presented in the present work is the shaping time of the DSSD energy amplifiers, which was set to be 0.5 μs. This means that the amplifiers take 0.5 μs to shape the signal received in the DSSDs in order to make an accurate energy measurement. Therefore, if a second signal is received within the shaping time, then the energy signals will pile up and a summed energy will be recorded. The consequences of the energy summing are discussed in the next section.

IV. DATA ANALYSIS

Data were acquired using the triggerless Total Data Readout (TDR) system [32] and were subsequently analysed using the GRAIN software package [33], which was specifically developed for use with TDR data. For α-particle spectroscopy, accurate energy calibrations of the DSSDs are very important. The calibrations were carried out using known energies of α particles emitted from evaporation residues implanted into the DSSDs, or in their decay chains. For the ^{18}O+^{208}Pb experiment, the α decays used were from ^{210}Po [E_α = 5304.33(7) keV], ^{220}Ra [E_α = 7453(7) keV], ^{222}Th [E_α = 7603(3) and 7986(3) keV], ^{219}Ra [E_α = 7678(3) keV], ^{213}Rn [E_α = 8088(8) keV], and ^{221}Th [E_α = 7732(2) 8144(2), and 8466(2) keV]. For the ^{20}Ne+^{208}Pb experiment, the same α-decays were used, with the exception of those from ^{220}Ra and ^{219}Ra. Due to more abundant statistics from the ^{18}O+^{208}Pb experiment, $\alpha\gamma$ coincidences were studied; for that experiment, the absolute efficiency for the detection of γ rays in the focal-plane clover HPGe detectors was determined by comparing the numbers of α particles in the DSSDs with numbers of detected $\alpha\gamma$ coincidences.

Signals recorded in the DSSDs were due either to the implantation of recoiling reaction products or scattered beam ions (henceforth referred to as *implants*) or due to the decays of implanted nuclei (*decays*). In assigning signals as decays, the correlation between the energy recorded by the DSSDs (E_{DSSD}) and the time-of-flight between signals in SAGE and signals in the DSSDs (t_{TOF}) was used. Two-dimensional gates on plots of these quantities were used to veto signals from being assigned as decays; these gates were centred on (t_{TOF}, E_{DSSD}) coordinates of (2.0 μs, 2.0 MeV) for the ^{18}O+^{208}Pb experiment and (1.4μs, 4.4 MeV) for the ^{20}Ne+^{208}Pb experiment. Once the discrimination between implants and decays had been achieved, specific conditions were applied to decay energies and times to select nuclei of interest. In the data from the ^{18}O+^{208}Pb experiment, the ^{218}Ra nuclei of interest were selected by requiring three signals in any one DSSD pixel, as follows: (i) an implant [at time t_0]; (ii) a decay corresponding to the α decay of ^{222}Th [at time t_1]; and (iii) a decay corresponding to the α decay of ^{218}Ra [at time t_2]. It was required that $t_1 - t_0 < 16$ ms [i.e. less that seven half-lives of ^{222}Th] and $t_2 - t_1 < 180$ μs [i.e. less that seven half-lives of ^{218}Ra]. No conditions were placed on the energies of the ^{222}Th α decays in the selection of ^{218}Ra nuclei. For the study of ^{220}Th from the ^{20}Ne+^{208}Pb experiment essentially the same method was used to select the ^{220}Th nuclei. However, the α decay required in step (ii) was from ^{224}U instead of ^{222}Th and in step (iii) ^{220}Th instead of ^{218}Ra. Also, in step (ii) the full energy of the α particle in the ^{224}U$\rightarrow^{220}$Th ground-state to ground-state decay [E_α = 8479(8) keV [34]] was required, due to contamination from ^{222}Th. Furthermore, it was required that $t_1 - t_0 < 2.77$ ms [i.e. less that seven half-lives of ^{224}U] and $t_2 - t_1 < 68$ μs [i.e. less that seven half-lives of ^{220}Th].

In the experimental set-up used here (designed for the purpose of recoil-decay tagging [35]) the detector (DSSD pixel) which records the implant is the same detector that records the subsequent decays of the implant. Use of the detector in this way has some important consequences. Firstly, the energies of the different events (implants and decays) in the detector can pile-up giving a summed energy signal, instead of a signal corresponding to a single event. The summed energy signal can be from an implant plus a decay or from a decay and a subsequent decay, and will be recorded when the time between events is comparable to the detector response time. Secondly, the α particles may not be fully contained within the detector, leading to partial energy deposition. Therefore, the energies recorded may be piled-up combinations of full and fractional parts of the energies of one or more events. This leads to complicated α-particle spectra, which need to be simplified and understood before α-particle energies and intensities can be extracted with confidence. These issues are discussed in more detail below. The energies of the evaporation residues in this work were low, and consequently the residues were implanted very close to the surface of the DSSDs; calculations suggest that the implantation depth is $\sim$0.4 μm [36]. If a nucleus implanted at this depth undergoes α decay, the full energy of the α particle will only be recorded if the α particle is emitted *into* the detector. If the α particle is emitted *out of* the detector, then only a small fraction of its energy will be deposited before the α particle leaves the detector material. In that case, there will be roughly equal probabilities ($\sim$50%) of detection of the full and partial energies.

In order to understand the energy summing and pile-up that is observed in the DSSDs, consideration has to be given to the processing time for each signal. In the methods used here, it is a requirement that there are two or more consecutive signals within the same detector (DSSD pixel) corresponding to an implant and at least one decay. If the implanted nucleus, or one of its decay products, has a half-life which is less than or comparable to the shaping time of the amplifier of the energy

signal, then the energies of the signals will pile up, giving a summed energy signal. As an example, consider a two-α decay chain $\alpha_1\alpha_2$ where the energy signals pile up. Each of the α particles can be either fully or partially recorded, so there are four possible values of the recorded energy, as follows: (i) partial energies for both α_1 and α_2 (PP); (ii) full energy of α_1 plus partial energy of α_2 (FP); (iii) partial energy of α_1 plus full energy of α_2 (PF); (iv) full energies for both α_1 and α_2 (FF). This is illustrated schematically in the upper part of Fig. 1. In the present work, one of the decay chains of interest is $^{222}_{90}$Th$\rightarrow^{218}_{88}$Ra$\rightarrow^{214}_{86}$Rn$\rightarrow^{210}_{84}$Po for which the relevant half-lives are as follows: $T_{1/2}(^{222}\text{Th})\simeq$2.0 ms [20]; $T_{1/2}(^{218}\text{Ra})\simeq$25 μs [24]; $T_{1/2}(^{214}\text{Rn})\simeq$270 ns [4]; and $T_{1/2}(^{210}\text{Po})\simeq$140 days [37]. The half-life of ^{214}Rn is shorter than the 0.5 μs shaping time. The energies of the α particles emitted from ^{218}Ra and ^{214}Rn therefore pile up, leading to a summed energy signal. The spectrum of these summed energy signals recorded in the DSSDs is shown in Fig. 1, with the selection of ^{218}Ra as described earlier. The four features in the spectrum discussed above are labelled (PP, FP, PF and FF).

The energy summing described above means that neither of the individual α-particle energies of ^{218}Ra or ^{214}Rn can be easily determined from the spectrum shown in Fig. 1. Such energy-summing issues have hampered earlier work; for example, it was explicitly noted in Ref. [21] that the measurement of the α-decay energy of ^{218}Ra was complicated by the summing with ^{214}Rn α decays. In the present work, use of the GREAT spectrometer has allowed this problem to be mitigated by applying a type of α-particle escape suppression, with the PIN-diode detectors acting as a suppression shield for the DSSDs. In essence, by choosing the time interval between the summed α-particle energy signal (in the DSSDs) and the escaped α-particle signal (in PIN-diode detectors) has enabled the individual ^{218}Ra α decays to be selected. The time of detection of the summed energy signal in the DSSDs (t^{sum}_{DSSD}) gives the time of the first (^{218}Ra) α decay; the time of detection of the escaping α particle (t^{escape}_{PIN}) can then be studied relative to this, such that Δt is defined as $\Delta t = t^{escape}_{PIN} - t^{sum}_{DSSD}$. Figure 2 shows DSSD energy spectra where a PIN-diode detector signal with $E > 500$ keV has been measured in delayed coincidence with the summed energy signals (shown in Fig. 1). Panel (a) has been incremented with the condition that $0 \leq \Delta t < 2.5$ μs, i.e. up to $\approx$10 ^{214}Rn half-lives. The spectrum shows both FP and PF peaks because this time interval will include escaping ^{218}Ra α particles [which have $\Delta t \simeq 0$] and escaping ^{214}Rn α particles which are emitted according to the ^{214}Rn half-life. Panel (b) is incremented with the condition 100 ns $< \Delta t < 2.5$ μs. This condition excludes the possibility of detecting an escaping ^{218}Ra α particle [$\Delta t \simeq 0$], so the PF distribution is removed. The time condition will also exclude some of the ^{214}Rn decays, so the part of the FP peak due to the partial energy of the ^{214}Rn α particles is reduced. This feature is further reduced in size on Panel (c) which has the condition 500 ns $< \Delta t < 2.5$ μs. For Panel (d), the condition 1.5 μs $< \Delta t < 2.5$ μs is applied which excludes essentially all of the escaping ^{214}Rn decays as they occur well after the amplifier shaping time (0.5 μs). This spectrum therefore only shows the full-energy peak associated with the ^{218}Ra α decay. From this spectrum, it is possible to make a measurement of the α-particle energy.

V. RESULTS

A. ^{218}Ra α-decay chain

The nucleus ^{218}Ra was produced as the α-decay daughter of ^{222}Th in the ^{18}O+^{208}Pb experiment. The cross section for the production of ^{222}Th was several millibarns, meaning that the ^{218}Ra data were relatively abundant. Using the methods described in the previous section, the energy of the α particle emitted in the ^{218}Ra$\rightarrow^{214}$Rn decay was measured to be 8381(4) keV, with a branching ratio b_α=99.88(6)%. The $\alpha\gamma$-coincidence spectra show that these α particles are only observed in random coincidence with background γ rays; for this reason, this α decay is assigned to populate the ground state of ^{214}Rn. From analysis of the time difference between ^{222}Th and ^{218}Ra α decays in the DSSDs, the half-life of ^{218}Ra was measured to be 25.99(10) μs.

In order to search for fine structure in the α decay of ^{218}Ra, $\alpha\gamma$-coincidence spectra were analysed. A two-dimensional $\alpha\gamma$-coincidence spectrum is shown in Fig. 3(a); the DSSD energy shown on the vertical axis is the α-particle summed energy that was shown in Fig. 1. The spectrum shown in Fig. 3(b) is the γ-ray projection of the spectrum of Panel (a). It is apparent that the γ ray with energy 695.0(2) keV is coincident with the four summed α-particle energy distributions. No other discrete γ-ray transitions are detected in coincidence with α particles, apart from the 511-keV annihilation γ ray. The energy of the 2^+_1 state in ^{214}Rn has previously been measured to be 693.6 keV [25, 38, 39]. The present data therefore suggest that the ^{218}Ra α particles which produce the summed α-particle energy distributions that are in coincidence with the 695-keV γ ray may be from a decay which directly populates the 2^+ state of ^{214}Rn. An attempt was made to measure the associated α-particle energy using the summed-energy signals in coincidence with the 695-keV γ ray. Unfortunately, it was not possible to identify any PIN-diode detector signals in the time interval of 1.5 to 2.5 μs after a DSSD signal, presumably due to low population.

Evidence that the α decay populates the 2^+ state of ^{214}Rn was, however, obtained by further scrutiny of the $\alpha\gamma$-coincidence data. Figure 3(c) shows the summed energy distributions (FP and PF) for the ^{218}Ra and ^{214}Rn α decays. Panel (d) shows the same data but with the additional requirement of coincidence with a 695-keV γ ray in the focal-plane clover HPGe detectors. The left-hand peak of Panel (c) and the main peak shown in Panel

(d) are both due to the detection of a full-energy ^{218}Ra α particle summed with a partial-energy ^{214}Rn α particle. If the decays corresponding to these peaks populate different final states then the energy difference between the peaks will relate to the energy difference between the final states. The energy difference between the peaks is 665(40) keV, as indicated on Panel (d). This is consistent with the expected α-particle energy difference of 682 keV, given the 2_1^+ excitation energy of 695 keV in ^{214}Rn, and gives an energy of 7715(40) keV for the α particle associated with the decay from the ground state of ^{218}Ra to the 2^+ state of ^{214}Rn. The branching ratio for this decay was measured to be $b_\alpha = 0.123(11)\%$.

Using the time differences between (^{218}Ra + ^{214}Rn) summed α-particle energy signals in the DSSDs and subsequent escaping (^{214}Rn) α-particle signals in the PIN-diode detectors, the half-life of the ^{214}Rn ground state has been measured to be 259(3) ns. This half-life result for ^{214}Rn is consistent with the previously measured values of 270(20) ns from Ref. [4] and 263(35) ns from Ref. [25].

B. ^{220}Th α-decay chain

In this work, the nucleus ^{220}Th was produced as the α-decay daughter of ^{224}U in the ^{20}Ne+^{208}Pb experiment. As ^{224}U was produced with a very small cross section of several hundred nanobarns, the amount of ^{220}Th data was limited. For this reason, the analysis techniques were first developed using the ^{218}Ra data from the same (^{20}Ne+^{208}Pb) experiment, which were produced with a far greater cross section, and which could be compared to the ^{218}Ra data from the other (^{18}O+^{208}Pb) experiment. In the ^{20}Ne+^{208}Pb experiment, the nucleus ^{218}Ra was produced as the α-decay daughter of ^{222}Th, which itself was produced by $\alpha 2n$ evaporation from the ^{228}U compound nucleus. Once the analysis methods were shown to work for ^{218}Ra, they could then be applied to ^{220}Th.

In order to measure the energies of the α particle emitted from nuclei implanted into the DSSDs, it was necessary to remove, or account for, the effect of energy summing. An attempt was made to select the non-summed DSSD energy signals by considering the DSSD signals that were followed by signals in the PIN-diode detectors, within specific time intervals. As such, two-dimensional plots were constructed with the DSSD energies plotted against the time, Δt, between the signal in the DSSDs and the signal in the PIN-diode detectors. This plot for ^{218}Ra, from the ^{20}Ne+^{208}Pb experiment, is shown in Fig. 4(a). It is clear that for low values of Δt, the energy distribution recorded by the DSSDs is wide, with counts spread over 1 MeV from 8500 keV up to 9500 keV or more. As Δt increases, the distribution gradually becomes more narrow until 1.35 μs, where a constant width of around 40 keV is maintained. It can therefore be assumed that with a time difference of more than 1.35 μs between the signals in the DSSDs and the PIN-diode detectors, the energy summing does not occur. The projection of the DSSD energies for times of $1.35\ \mu s \leq \Delta t \leq 2.5\ \mu s$ is shown in Fig. 4(b). The counts clearly form a well-defined peak with a centroid at an energy of 8382(5) keV, which is consistent with the value from the ^{18}O+^{208}Pb experiment.

Spectra from the analysis of ^{220}Th from the ^{20}Ne+^{208}Pb experiment are shown in the lower panels of Fig. 4. Panel (c) and (d) are analogous to Panels (a) and (b). It is immediately apparent that the number of counts is significantly reduced in this case. Nonetheless, for $\Delta t \geq 1.35\ \mu$s, there are two counts which have very similar energies; the projection of the DSSD energies for times of $1.35\ \mu s \leq \Delta t \leq 2.5\ \mu s$ is shown in Fig. 4(c), where two counts can be seen in the same channel with zero background. From these counts a value of 8818(13) keV for the α-particle energy for the ^{220}Th ground-state decay was found. For comparison, the DSSD energy signals with $0 \leq \Delta t \leq 2.5\ \mu$s are shown in Fig. 4(e).

From the time differences between the ^{224}U and ^{220}Th α-decay signals in the DSSDs, the half-life of the ^{220}Th ground state has been measured to be 10.4(4) μs. This is consistent with the previously reported values of 12^{+4}_{-3} μs [26] and 9.7(6) μs [7]. From the time differences between (^{220}Th + ^{216}Ra) summed α-particle energy signals in the DSSDs and subsequent escaping (^{216}Ra) α-particle signals in the PIN-diode detectors, the half-life of the ^{216}Ra ground state was measured to be 161(11) ns. This is lower than the previously reported value of 182(10) ns [27].

VI. DISCUSSION

A. Comparison with previous measurements

In the present work, the ground-state to ground-state ^{218}Ra$\rightarrow^{214}$Rn α-particle energy has been measured to be 8381(4) keV. This is consistent with the values of 8385(10) keV measured by Valli *et al.* [4] and 8392(8) keV measured by Torgerson *et al.* [6]. The value of 8480(20) keV measured by Kim *et al.* [21] is around 100 keV higher than the values measured here and in Refs. [4, 6]; the higher energy in that work is likely to be due to the method of inferring α-particle energies from summed-energy distributions. Indeed, the energy of the α particle in the ^{214}Rn decay was reported in Ref. [21] as 9150(20) keV, compared with 9035(10) keV measured by Valli *et al.* [4] and 9040(20) keV measured by Torgerson *et al.* [6]. The results of Refs. [4, 6] were not affected by α-particle energy summing as the decaying nucleus was not implanted into the α-particle detector. In the present work, the half-life of ^{218}Ra has been measured to be 25.99(10) μs. This is not consistent with the value measured by Valli *et al.* of 14(2) μs [4], but is in agreement with the values of 25.6(11) μs measured by Toth *et al.* [22], 26(2) μs measured by Wieland *et al.* [23] and

25.2(3) μs measured by Kuusiniemi *et al.* [24]. As reported by Toth *et al.* [22] the half-life of $\sim$25 μs gives an α-decay reduced width which is in agreement with systematics.

In the present work, the value of the α-particle energy from the ground-state to ground-state ^{220}Th$\rightarrow^{216}$Ra decay has been measured to be 8818(13) keV. This value is higher than the previous measurement of 8790(20) keV reported in Ref. [7]. This previous measurement of the energy required the implantation of the recoiling ^{220}Th nuclei into a carbon catcher foil at the target position. The α-particle energies were then measured and a correction was applied for the energy loss in the catcher foil. It is possible that the correction introduced a systematic uncertainty in the α-particle energies.

B. Hindrance factors and systematics

In the study of α-decay and its fine structure, it is often useful to define the *hindrance factor*. This is defined as the ratio of the experimental and calculated partial half-lives; the experimental half-life is determined using the measured branching ratio and half-life values, and the calculated half-life is determined using a simple model of a preformed α particle in the potential of the daughter nucleus. This definition of the hindrance factor removes the energy dependence of the decay and can give a measure of the overlap of the wavefunctions of initial and final states. Using the theoretical partial half-life calculated as described by Preston [40] a hindrance factor of 8.36(17) is given for the new fine-structure α decay from the ^{218}Ra ground state to the 2_1^+ state in ^{214}Rn. This is relative to a hindrance factor of 1 for the decay to the ^{214}Rn ground state.

The properties of the new fine structure α decay in ^{218}Ra can be compared to experimental systematics. In Ref. [41], a universal rule is established which relates the hindrance factors of fine-structure α decays to the excitation energies of the populated states. This relation has recently been tested by Delion and Dumitrescu in systematic analyses of α-decay fine structure in a wide range of nuclei [2, 3]. In these studies the model-independent variable of α-decay intensity, I_J, is favoured over the hindrance factor; this is defined as the logarithm of the ratio between the decay widths to the ground and excited states. The new results presented here are found to be in good agreement with the linear relationship established between the α-decay intensities to 2_1^+ states and the excitation energies of the states. The new fine-structure in the α decay of ^{218}Ra identified in this work extends the systematics to one of the highest known 2^+ energies (695 keV) populated by α decay of even-even nuclei.

Hindrance factors to low-lying excited states can be used as a measure of the overlap of the wavefunctions for ground and excited states, and therefore can be used as a measure of collectivity. As such, recent studies by Bucurescu and Zamfir: [42, 43] have analysed the systematics of the α-decay hindrance factors and intensities to low-lying excited states in even-even trans-lead nuclei, in relation to variables which are indicative of nuclear collectivity. This analysis enabled the onset of collectivity to be traced from the doubly-magic ^{208}Pb nucleus towards the collective rotational nuclei at mid-shell. With just two neutrons and four protons above ^{208}Pb, the nucleus ^{214}Rn is not considered to be collective. The large hindrance factor from the present work is consistent with the systematics for less collective nuclei.

C. Applications of the new methods

The techniques used in this work offer complimentary methods to study short-lived and weak α-decay branches from nuclei implanted into a detector in which the daughter products have very short half-lives. Using these methods, it could therefore be possible to identify fine structure in the other $N = 130$ nuclei $^{216}_{86}$Rn, $^{217}_{87}$Fr, $^{219}_{89}$Ac, $^{220}_{90}$Th, $^{221}_{91}$Pa, $^{222}_{92}$U, and $^{223}_{93}$Np. The ^{218}Ra$\rightarrow^{214}$Rn fine structure reported here is the only known example. The methods would also allow short-lived nuclei produced with low cross sections relative to other background α emitters to be studied. The methods used here give accurate α-particle energies from implanted nuclei, free from energy-summing effects, so it could also be used to remeasure the α-particle energies of the ground-state to ground-state decays of the other $N = 130$ nuclei which have previously be measured using other techniques which may be prone to large or systematic uncertainties.

VII. SUMMARY

Alpha-decay spectroscopy of the $N = 130$ isotones ^{218}Ra and ^{220}Th has been carried out. The nucleus ^{218}Ra was produced following the α decay of ^{222}Th. The energy of the α particle emitted in the ^{218}Ra$\rightarrow^{214}$Ra decay has been measured to be 8381(4) keV. In addition, fine structure in the α decay of ^{218}Ra, populating the 695-keV 2_1^+ state in ^{214}Rn has been observed with energy $E_\alpha = 7715(40)$ keV and branching ratio $b_\alpha = 0.123(11)\%$. The observation of the new α-decay fine structure was achieved using $\alpha\gamma$ coincidence measurements. The nucleus ^{220}Th was produced following the α decay of ^{224}U. The energy of the α particle emitted in the ^{220}Th$\rightarrow^{216}$Ra decay has been measured to be 8818(13) keV. These measurements have been made possible by the development of methods to overcome the problem of energy summing in α-particle spectroscopy from nuclei implanted into a detector, which happens when the α decay of the subsequent nucleus occurs within the amplifier shaping time. Several potential uses of the

new data analysis methods have been proposed.

This work is supported in part by the STFC (UK) under grants ST/J000183/2, ST/L005808/1, EP/E02551x1/1, and ST/L005794/1; by the EU 7th Framework Programme, Integrating Activities Transnational Access, project No.262010 (ENSAR); by the Academy of Finland under the Finnish Centre of Excellence Programme (Nuclear and Accelerator Based Physics Programme at JYFL); by the Slovak Research and Development Agency under Contract No. APVV-15-0225; and by the Slovak grant agency VEGA (Contract No. 2/0129/17); and the project ITMS code 26210120023, supported by the Research and Development Operational Programme funded by ERDF (30 %). The authors acknowledge support of Gammapool for use of the Jurogam detectors. EP, JFS and MSc acknowledge support of the Scottish Universities Physics Alliance (SUPA).

TABLE I: Summarised details of the experiments.

	Beam			Target		
Expt	Nucleus	Energy (MeV)	Intensity (pnA)	Nucleus	Thickness (mg cm^{-2})	Duration (hours)
1	^{18}O	95	18	^{208}Pb	0.45	157
2(a)	^{20}Ne	109	26	^{208}Pb	0.45	259
2(b)	^{20}Ne	109	23	^{208}Pb	0.25	39

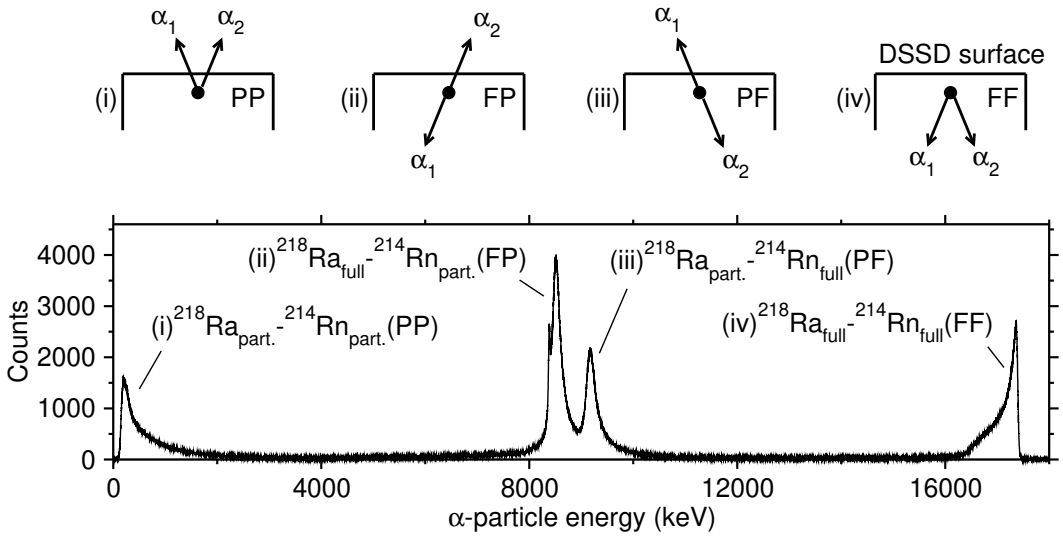

FIG. 1: Spectrum showing summed α-particle energies from the ^{218}Ra$\rightarrow^{214}$Rn$\rightarrow^{210}$Po decay chain, selected following an implant and a ^{222}Th α decay, from the ^{18}O+^{208}Pb experiment. The energy range is from 0 to 18 MeV, which includes all full and partial summed energies in the decay chain; each feature in the spectrum is labelled as the sum of a full (F) or partial (P) ^{218}Ra or ^{214}Rn, α-particle energy. Schematic representations of the four possible events in the DSSD, corresponding to each of the four features in the spectrum, are shown above the main panel.

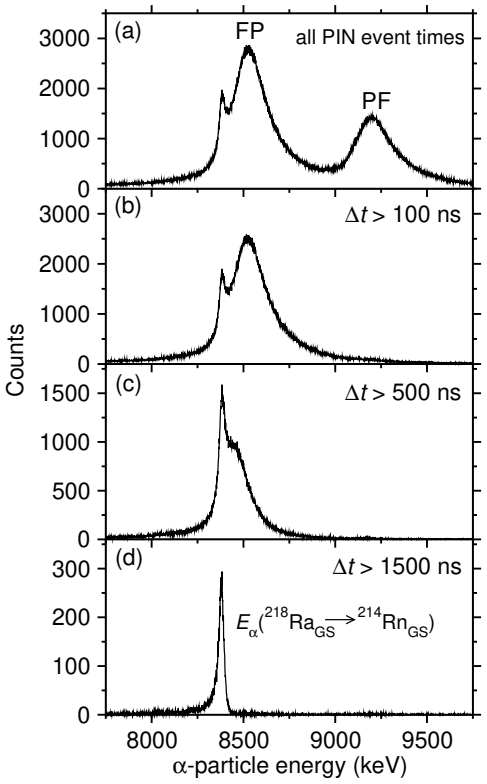

FIG. 2: Spectra of the summed α-particle energies measured in the DSSDs from the ^{218}Ra$\rightarrow^{214}$Rn$\rightarrow^{210}$Po decay chain, selected following an implant followed by a ^{222}Th α decay, with the additional requirement of a PIN-diode detector signal measured in delayed coincidence. The data are taken from the ^{18}O+^{208}Pb experiment. Panel (a) shows the spectrum where the PIN-diode detector signal is measured in coincidence with, or up to 2.5 μs after, the DSSD signal. Spectra in panels (b), (c) and (d) require that the PIN-diode detector signal arrives at least 100 ns, 500 ns, and 1.5 μs after the DSSD signal, respectively.

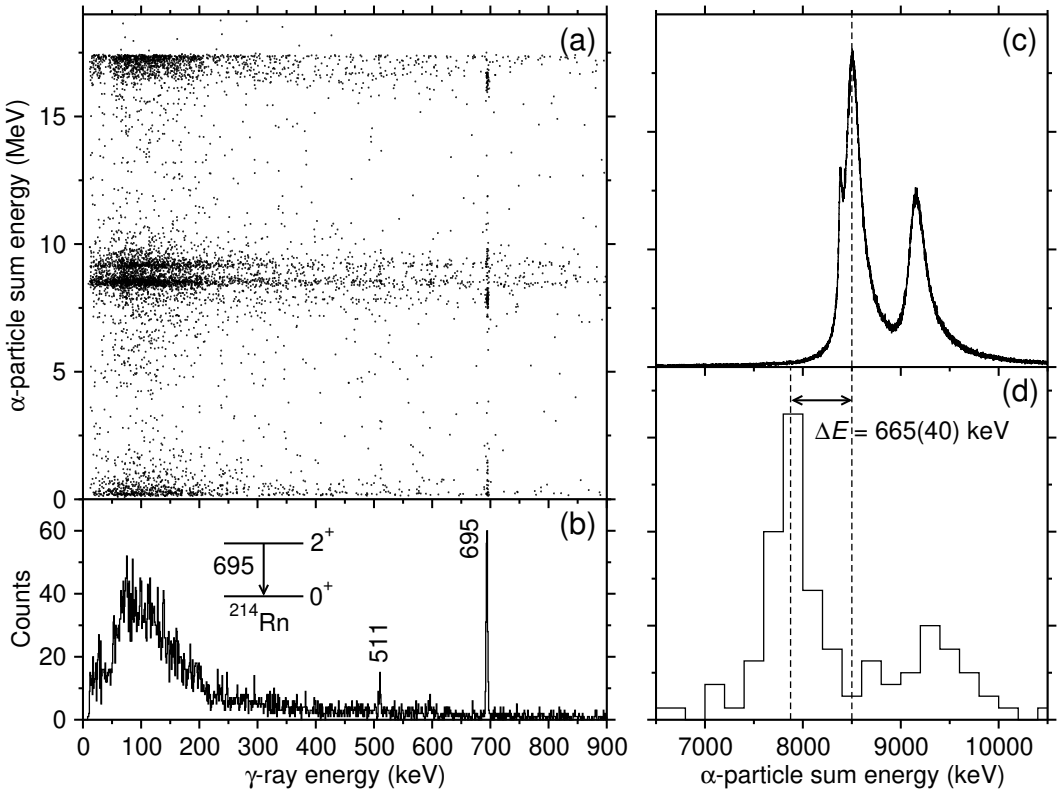

FIG. 3: Spectra from the $\alpha\gamma$-coincidence analysis, in the data from the ^{18}O+^{208}Pb experiment. Panel (a) shows a two-dimensional plot of $\alpha\gamma$ coincidences following the α decay of ^{218}Ra. Panel (b) shows the full projection of γ-ray energies from Panel (a). Panel (c) shows the summed α-particle energies for the ^{218}Ra$\rightarrow^{214}$Rn$\rightarrow^{210}$Po α-decay chain. Panel (d) shows the same data as (c) but with the additional requirement of a coincident 695-keV γ ray in the clover HPGe detectors at the focal plane of RITU.

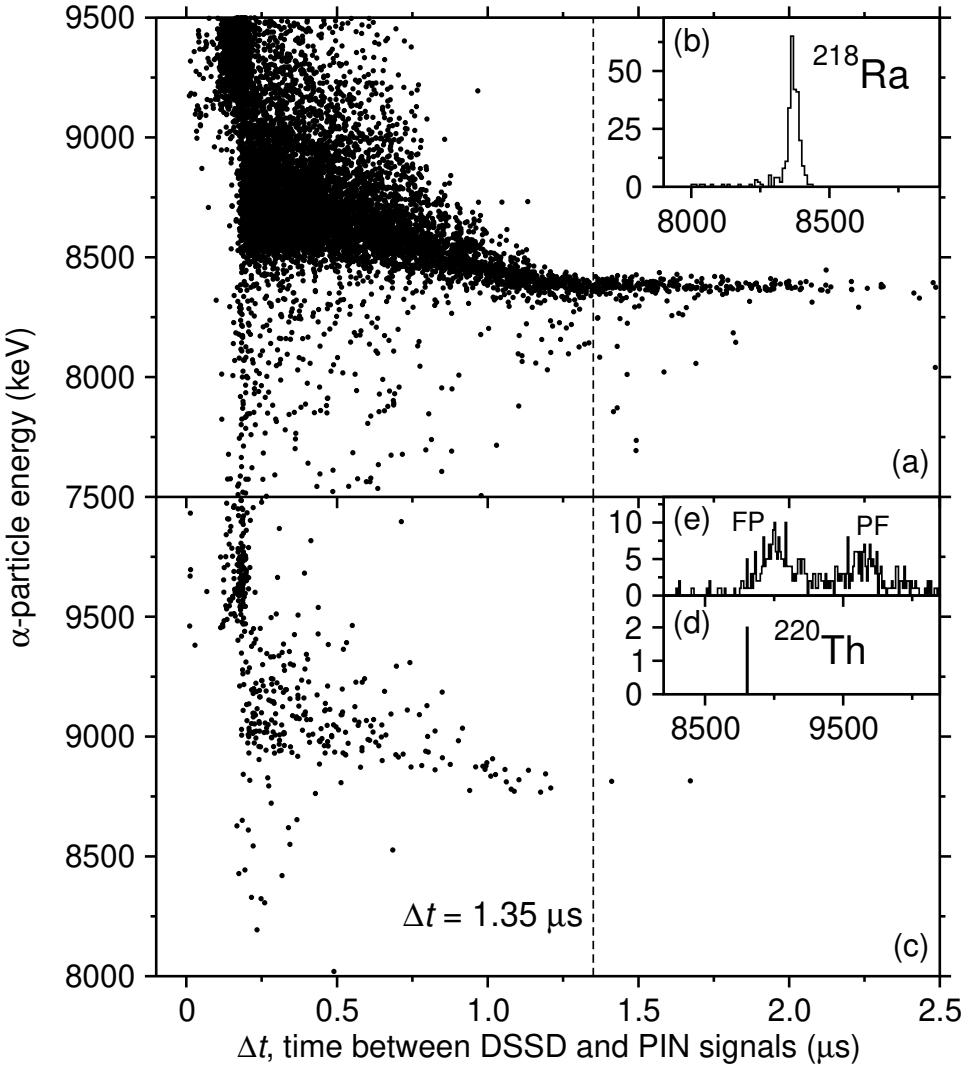

FIG. 4: Spectra showing the relationship between energies measured in the DSSDs that are followed by a signal in the PIN-diode detectors, and the time Δt between the signals in the DSSDs and the PIN-diode detectors, for values of Δt up to 2.5 μs. Results are taken from the ^{20}Ne+^{208}Pb experiment. Panel (a) shows the energy measured by the DSSD focused on the (^{218}Ra + ^{214}Rn) summed-energy region against Δt, and Panel (b) shows the projected energy measured for $1.35 \leq \Delta t \leq 2.5$ μs. Panel (c) shows the energy measured by the DSSD focused on the (^{220}Th + ^{216}Ra) summed-energy region, and Panel (d) shows the energy measured for $1.35 \leq \Delta t \leq 2.5$ μs. Panel (e) is the same as Panel (d) but for $0 \leq \Delta t \leq 2.5$ μs, and is shown for comparison with Panel (d). The vertical dashed line shows $\Delta t = 1.35$ μs; for $\Delta t > 1.35$ μs, the energy-summing effects are no longer observed.

[1] Y. A. Akovali, Nucl. Data Sheets **84**, 1 (1998).
[2] D. S. Delion and A. Dumitrescu, Phys. Rev. C **92**, 021303(R) (2015).
[3] D. S. Delion and A. Dumitrescu, At. Data Nucl. Data Tables **101**, 1 (2015).
[4] K. Valli, E. K. Hyde and J. Borggreen, Phys. Rev. C **1**, 2115 (1970).
[5] J. Borggreen, K. Valli and E. K. Hyde, Phys. Rev. C **2**, 1841 (1970).
[6] D. F. Torgerson and R. D. Macfarlane, Nucl. Phys. A **149**, 641 (1970).
[7] O. Hausser, W. Witthuhn, T. K. Alexander, A. B. McDonald, J. C. D. Milton and A. Olin, Phys. Rev. Lett. **31**, 323 (1973).
[8] R. Hingmann, H.-G. Clerc, C.-C. Sahm, D. Vermeulen, K.-H. Schmidt and J. C. Keller, Z. Phys. A **313**, 141 (1983).
[9] H. Miyatake, T. Nomura, S. Kubono, J. Tanaka, M. Oyaizu, H. Okawa, N. Ikeda, K. Sueki, H. Kudo *et al.*, Nucl. Phys. A **501**, 557 (1989).
[10] R. Grzywacz, Nucl. Instrum. Methods Phys. Res., Sect. B **204**, 649 (2003).
[11] S. N. Liddick, R. Grzywacz, C. Mazzocchi, R. D. Page, K. P. Rykaczewski, J. C. Batchelder, C. R. Bingham, I. G. Darby, G. Drafta *et al.*, Phys. Rev. Lett. **97**, 082501 (2006).
[12] S. N. Liddick, R. Grzywacz, C. Mazzocchi, R. D. Page, K. P. Rykaczewski, J. C. Batchelder, C. R. Bingham, I. G. Darby, G. Drafta *et al.*, Eur. Phys. J.-Spec. Top. **150**, 131 (2007).
[13] I. G. Darby, R. K. Grzywacz, J. C. Batchelder, C. R. Bingham, L. Cartegni, C. J. Gross, M. Hjorth-Jensen, D. T. Joss, S. N. Liddick *et al.*, Phys. Rev. Lett. **105**, 162502 (2010).
[14] K. Auranen, D. Seweryniak, M. Albers, A. D. Ayangeakaa, S. Bottoni, M. P. Carpenter, C. J. Chiara, P. Copp, H. M. David *et al.*, Phys. Rev. Lett. **121**, 182501 (2018).
[15] J. Khuyagbaatar, A. Yakushev, Ch. E. Dullmann, D. Ackermann, L. L. Andersson, M. Block, H. Brand, D. M. Cox, J. Even *et al.*, Phys. Rev. Lett. **115**, 242502 (2015).
[16] M. D. Sun, Z. Liu, T. H. Huang, W. Q. Zhang, J. G. Wang, X. Y. Liu, B. Ding, Z. G. Gan, L. Ma *et al.*, Phys. Lett. B **771**, 303 (2017).
[17] P. A. Butler and W. Nazarewicz, Rev. Mod. Phys. **68**, 349 (1996).
[18] G. A. Leander and R. K. Sheline, Nucl. Phys. A **413**, 375 (1984).
[19] R. J. Poynter, P. A. Butler, G. D. Jones, R. J. Tanner, C. A. White, J. R. Hughes, S. M. Mullins, R. Wadsworth, D. L. Watson *et al.*, J. Phys. G **15**, 449 (1989).
[20] E. Parr, J. F. Smith, P. T. Greenlees, M. Smolen, P. Papadakis, K. Auranen, R. Chapman, D. M. Cullen, T. Grahn *et al.*, Phys. Rev. C **94**, 014307 (2016).
[21] H. J. Kim, K. S. Toth, M. N. Rao and J. W. McConnell, Nucl. Instrum. Methods Phys. Res., Sect. A **249**, 386 (1986).
[22] K. S. Toth, H. J. Kim, M. N. Rao and R. L. Mlekodaj, Phys. Rev. Lett. **56**, 2360 (1986).
[23] M. Wieland, J. Fernandez Niello, B. von Fromberg, F. Riess, M. Aiche, A. Chevallier, J. Chevallier, N. Schulz, J. C. Sens *et al.*, Phys. Rev. C **46**, 2628 (1992).
[24] P. Kuusiniemi, J. F. C. Cocks, K. Eskola, P. T. Greenlees, K. Helariutta, P. Jones, R. Julin, S. Juutinen, H. Kankaanpaa *et al.*, Acta Phys. Pol. B **32**, 1009 (2001).
[25] G. D. Dracoulis, A. P. Byrne, A. E. Stuchbery, R. A. Bark and A. R. Poletti, Nucl. Phys. A **467**, 305 (1987).
[26] A. N. Andreev, D. D. Bogdanov, A. V. Eremin, A. P. Kabachenko, O. N. Malyshev, G. M. Ter-Akopyan and V. I. Chepigin, Sov. J. Nucl. Phys. **53**, 554 (1991).
[27] T. Nomura, K. Hiruta and T. Inamura, Nucl. Phys. A **217**, 253 (1973).
[28] J. Pakarinen, P. Papadakis, J. Sorri, R.-D. Herzberg, P. T. Greenlees, P. A. Butler, P. J. Coleman-Smith, D. M. Cox, J. R. Cresswell *et al.*, Eur. Phys. J. A **50**, 53 (2014).
[29] M. Leino, Nucl. Instrum. Methods Phys. Res., Sect. B **126**, 320 (1997).
[30] J. Uusitalo, P. Jones, P. Greenlees, P. Rahkila, M. Leino, A. N. Andreyev, P. A. Butler, T. Enqvist, K. Eskola *et al.*, Nucl. Instrum. Methods Phys. Res., Sect. B **204**, 638 (2003).
[31] R. D. Page, A. N. Andreyev, D. E. Appelbe, P. A. Butler, S. J. Freeman, P. T. Greenlees, R.-D. Herzberg, D. G. Jenkins, G. D. Jones *et al.*, Nucl. Instrum. Methods Phys. Res., Sect. B **204**, 634 (2003).
[32] I. H. Lazarus, D. E. Appelbe, P. A. Butler, P. J. Coleman-Smith, J. R. Cresswell, S. J. Freeman, R.-D. Herzberg, I. Hibbert, D. T. Joss *et al.*, IEEE Trans. Nucl. Sci. **48**, 567 (2001).
[33] P. Rahkila, Nucl. Instrum. Methods Phys. Res., Sect. A **595**, 637 (2008).
[34] A. Lopez-Martens, K. Hauschild, K. Rezynkina, O. Dorvaux, B. Gall, F. Dechery, H. Faure, A. V. Yeremin, M. L. Chelnokov *et al.*, Eur. Phys. J. A **50**, 132 (2014).
[35] E. S. Paul, P. J. Woods, T. Davinson, R. D. Page, P. J. Sellin, C. W. Beausang, R. M. Clark, R. A. Cunningham, S. A. Forbes *et al.*, Phys. Rev. C **51**, 78 (1995).
[36] J. F. Ziegler, M. D. Ziegler and J. P. Biersack, Nucl. Instrum. Methods Phys. Res., Sect. B **268**, 1818 (2010).
[37] M. L. Curtis, Phys. Rev. **92**, 1489 (1953).
[38] Y. Gono, K. Hiruta, T. Nomura, M. Ishihara, H. Utsunomiya, T. Sugitate and K. Ieki, J. Phys. Soc. Jpn. **50**, 377 (1981).
[39] T. Lonnroth, D. Horn, C. Baktash, C. J. Lister and G. R. Young, Phys. Rev. C **27**, 180 (1983).
[40] M. A. Preston, Phys. Rev. **71**, 865 (1947).
[41] D. S. Delion, Phys. Rev. C **80**, 024310 (2009).
[42] D. Bucurescu and N. V. Zamfir, Phys. Rev. C **86**, 067306 (2012).
[43] D. Bucurescu and N. V. Zamfir, Rom. J. Phys. **57**, 69 (2012).